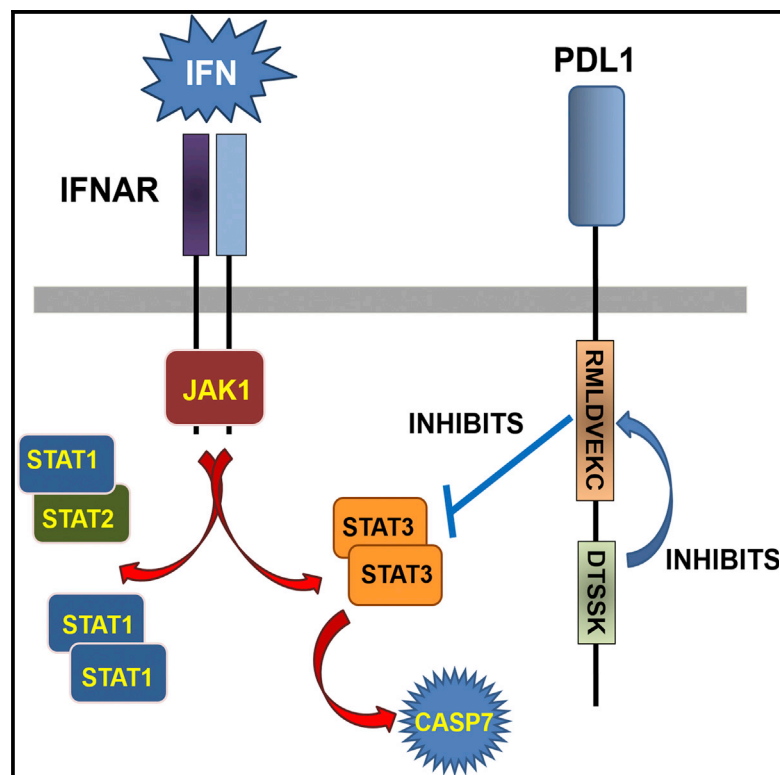# PDL1 Signals through Conserved Sequence Motifs to Overcome Interferon-Mediated Cytotoxicity

Graphical Abstract

Authors

Maria Gato-Cañas, Miren Zuazo, Hugo Arasanz, ..., Karine Breckpot, Grazyna Kochan, David Escors

Correspondence

grazyna.kochan@navarra.es (G.K.), d.escors@ucl.ac.uk (D.E.)

In Brief

Gato-Cañas et al. find that PDL1 protects cancer cells from interferon toxicity by counteracting interferon signaling through the activities of two non-classical conserved motifs. Human cancers acquire somatic mutations within these motifs that enhance PDL1 anti-interferon activities, favoring tumor progression.

Highlights

- PDL1 expression represents a direct defense barrier against IFN toxicity

- PDL1 contains non-classical conserved signal transduction motifs

- PDL1 signaling motifs as hotspots for hyperactivating somatic mutations in cancer

- Interfering with PDL1 signaling motifs sensitizes cancer cells to IFN cytotoxicity

CrossMark

CellPress

PDL1 Signals through Conserved Sequence Motifs to Overcome Interferon-Mediated Cytotoxicity

Maria Gato-Cañas,[1,7] Miren Zuazo,[1,7] Hugo Arasanz,[1,2,7] Maria Ibañez-Vea,[1,7] Laura Lorenzo,[1]
Gonzalo Fernandez-Hinojal,[1,2] Ruth Vera,[2] Cristian Smerdou,[3] Eva Martisova,[3] Imanol Arozarena,[1] Claudia Wellbrock,[4]
Diana Llopiz,[3] Marta Ruiz,[3] Pablo Sarobe,[3] Karine Breckpot,[5] Grazyna Kochan,[1,8,*] and David Escors[1,6,8,9,*]
[1]Department of Oncology, Navarrabiomed-Biomedical Research Centre, IdiSNA, 31008 Pamplona, Navarra, Spain
[2]Department of Oncology, Complejo Hospitalario de Navarra, IdiSNA, 31008 Pamplona, Navarra, Spain
[3]Center for Applied Medical Research (CIMA), University of Navarra, IdiSNA, Avenida Pio XII, 55, 31008 Pamplona, Spain
[4]Division of Molecular and Clinical Cancer Sciences, The University of Manchester, Oxford Road, M13 9PL Manchester, UK
[5]Department of Biomedical Sciences, Vrije Universiteit Brussels, Laarbeeklaan 103/E, 1090 Jette, Brussels, Belgium
[6]Division of Infection and Immunity, Rayne Institute, University College London, WC1E 6JF London, UK
[7]These authors contributed equally
[8]Senior author
[9]Lead Contact
*Correspondence: grazyna.kochan@navarra.es (G.K.), d.escors@ucl.ac.uk (D.E.)
http://dx.doi.org/10.1016/j.celrep.2017.07.075

SUMMARY

PDL1 blockade produces remarkable clinical responses, thought to occur by T cell reactivation through prevention of PDL1-PD1 T cell inhibitory interactions. Here, we find that PDL1 cell-intrinsic signaling protects cancer cells from interferon (IFN) cytotoxicity and accelerates tumor progression. PDL1 inhibited IFN signal transduction through a conserved class of sequence motifs that mediate crosstalk with IFN signaling. Abrogation of PDL1 expression or antibody-mediated PDL1 blockade strongly sensitized cancer cells to IFN cytotoxicity through a STAT3/caspase-7-dependent pathway. Moreover, somatic mutations found in human carcinomas within these PDL1 sequence motifs disrupted motif regulation, resulting in PDL1 molecules with enhanced protective activities from type I and type II IFN cytotoxicity. Overall, our results reveal a mode of action of PDL1 in cancer cells as a first line of defense against IFN cytotoxicity.

INTRODUCTION

Programmed death 1 ligand 1 (PDL1) is a member of the B7 family of co-stimulatory/co-inhibitory molecules expressed by a wide variety of cell types, including tumors (Sharpe et al., 2007). PDL1 is a transmembrane protein consisting of an immunoglobulin-like extracellular part, followed by a transmembrane domain and a short intracytoplasmic domain. Programmed death 1 (PD1) is its prototypical receptor, which is expressed mainly by effector immune cells such as B and T cells (Freeman et al., 2000; Zak et al., 2015). However, PDL1 can also bind CD80 (Butte et al., 2007). The physiological role of PDL1 is to maintain peripheral tolerance and contribute to antigen presentation to T cells by dendritic cells (Karwacz et al., 2011; Sharpe et al.,

2007). In neoplastic conditions, PDL1 tumor expression strongly correlates with increased progression and poor prognosis, being an indicator of resistance to conventional treatments such as chemotherapy and radiotherapy.

It is widely accepted that PDL1 protects cancer cells by engaging with PD1 expressed on the surface of activated cytotoxic T cells (Fife et al., 2009). This engagement is strongly inhibitory to T cells and leads to decreased effector activities. As a consequence, PDL1-engaged PD1 in T cells interferes with the T cell receptor (TCR) signalosome stopping T cell cytotoxic activities and production of cytokines such as interferons (IFNs) (Fife et al., 2009; Karwacz et al., 2011). Recent evidence suggests that PDL1 can activate intrinsic signals in the absence of PD1 that enhance cell proliferation and survival through the inhibition of autophagy and mTOR activation (Clark et al., 2016; Chang et al., 2015). However, in contrast to PD1, there is still very little evidence for specific signal transduction events induced by PDL1. No obvious sequence motifs in the intracytoplasmic domain with signal transduction capacities have been either predicted or identified so far (Azuma et al., 2008).

PDL1/PD1 blockade therapy has achieved unprecedented therapeutic clinical success for a variety of cancers, including melanoma. PDL1/PD1-blocking antibodies cause the recovery of T cell anti-tumor cytotoxicity and production of IFNs that inhibit tumor cell growth and survival. Therefore, a significant number of treated patients experience long-lasting anti-tumor responses (Hodi et al., 2016). However, a large number of patients are still intrinsically resistant to anti-PDL1/PD1 therapy or exhibit tumor progression after a period of therapeutic responses. Recently, it has been shown that inactivating mutations in JAK1, JAK2, and β2-microglobulin genes in cancer cells are responsible for primary and acquired resistance to anti-PD1 therapy in a cohort of cancer patients (Shin et al., 2017; Zaretsky et al., 2016). As IFN signals are potent transcriptional transactivators of PDL1, these mutations inhibited PDL1 upregulation in cancer cells. The authors proposed that the loss of PDL1 upregulation abrogated the antitumor efficacy of PDL1/PD1 blockade in these patients (Sharma et al., 2017).
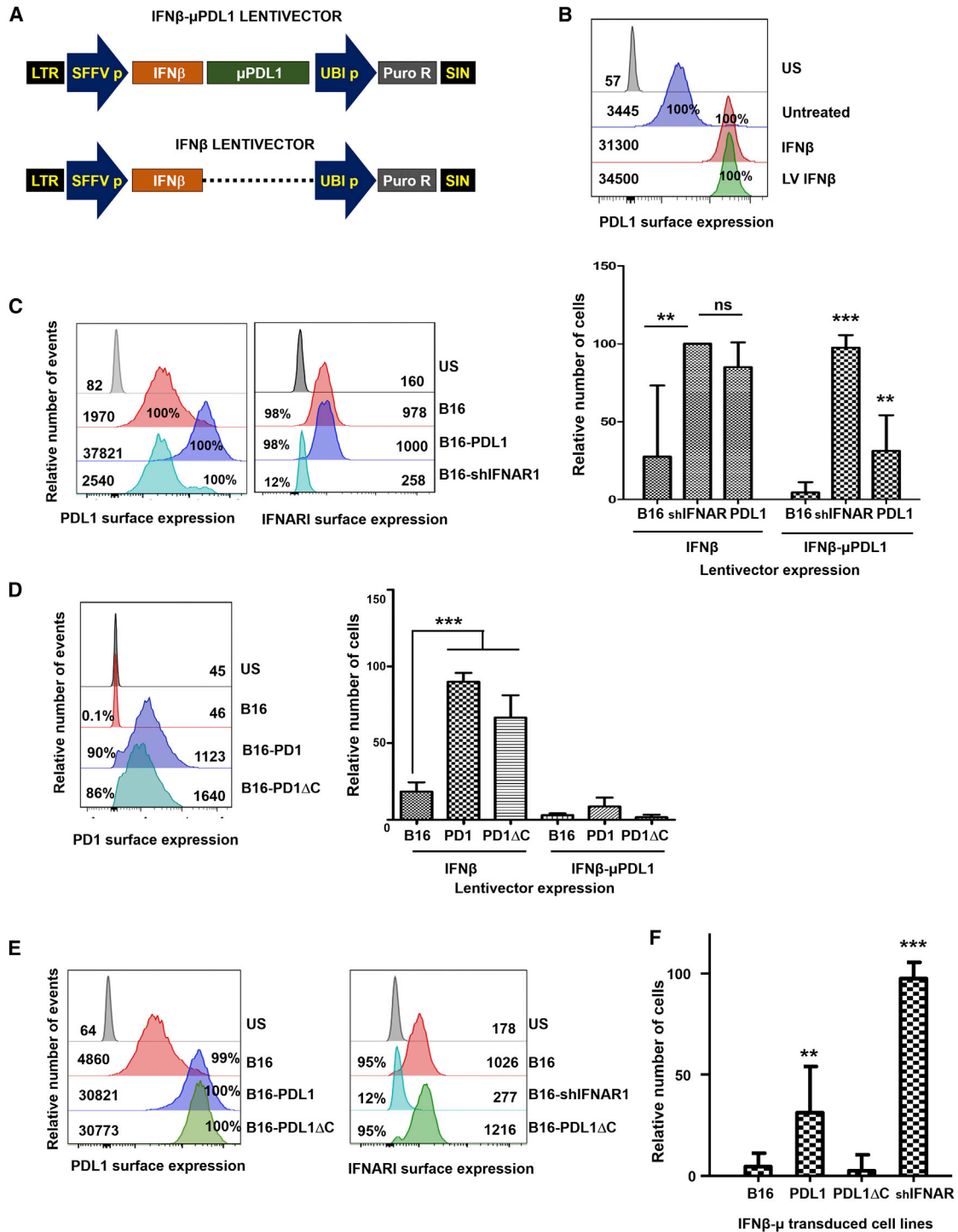
Figure 1. PDL1 Protects Melanoma Cells from IFNβ Toxicity

(A) Lentivector expression vectors used in the studies. LTR, long terminal repeats; SFFV, spleen focus-forming virus promoter; μPDL1, microRNA targeting murine PDL1; UBIp, ubiquitin promoter; PuroR, gene conferring puromycin resistance.

(B) Expression of surface PDL1 in B16 cells treated with recombinant IFNβ or transduced with the IFNβ-expressing lentivector. Data are shown as flow cytometry histogram plots. Numbers and percentages indicate mean fluorescent intensities and percentage of positive cells compared to the unstained (US) control.

(C) Left: flow cytometry histograms for PDL1 or IFNAR1 surface expression (as indicated) in the B16 cell lines as shown on the right of the histograms. Numbers and percentages indicate mean fluorescent intensities and percentage of positive cells. Right: bar graphs representing the mean relative number of cells with

(legend continued on next page)

Here, we demonstrate that PDL1 expression represents a direct line of defense for cancer cells by transducing signals that counteract IFN signal transduction within cancer cells. Moreover, we demonstrate that the PDL1 intracytoplasmic domain is essential for its protective functions through the activity of regulatory non-classical signal transduction motifs.

RESULTS

IFNβ Expression Coupled to PDL1 Silencing Is Lethal to Melanoma Cells

To engineer an immunogenic cell-based cancer vaccine, we attempted to generate a B16F10 melanoma cell line with silenced PDL1 that would secrete IFNβ. To achieve this, we cloned the IFNβ gene into a lentivector expressing a PDL1-targeted microRNA (μPDL1) and a puromycin selection gene previously described (Karwacz et al., 2011; Liechtenstein et al., 2014a) (Figure 1A). Strikingly, although puromycin-resistant cells could be obtained, these cells died within 1 or 2 weeks of culture. To identify the component conferring lethality, the IFNβ gene was expressed with or without μPDL1 (Figure 1A). Interestingly, it was possible to generate B16 cell lines expressing high levels of secreted IFNβ (6 ng/mL) only in the absence of μPDL1. As these cells had very high surface PDL1 protein expression (Figure 1B), this indicated that PDL1 upregulation could be an adaptation to survival from sustained IFNβ signaling. These results suggested that cancer cells may utilize PDL1 expression to negatively regulate IFN signal transduction. To confirm that the toxicity associated with PDL1 silencing was mediated through enhanced IFNβ signaling, B16 cells with a silenced type I IFN receptor (B16-IFNAR1[KD]) were generated using lentivector delivery of shRNA. Additionally, B16 cells overexpressing a PDL1 mutant with reduced complementarity to the μPDL1 (B16-PDL1) were also generated to strengthen PDL1 signaling (Figure 1C). B16-IFNAR1[KD] cells proliferated well regardless of whether they expressed IFNβ or IFNβ-μPDL1, confirming that lethality was conferred by IFN signal transduction (Figure 1C). Importantly, PDL1 overexpression in B16 cells overcame the inhibitory effects of IFNβ and the lethality of the IFNβ-μPDL1 combination (Figure 1C). Type I IFN receptor is a homodimer of IFNAR1 and IFNAR2 molecules, of which IFNAR1 is essential for signal transduction (Ragimbeau et al., 2003). As B16-PDL1 cells showed levels of surface IFNAR1 and IFNAR2 expression comparable to unmodified B16 cells (Figure 1C and not depicted), we concluded that PDL1 interfered with IFNβ signal transduction but did not cause IFNAR downmodulation.

PDL1 Signal Transduction Counteracts IFNβ Toxicity

To test whether the engagement of PDL1 with its receptor PD1 would deliver a protective signal against IFNβ cytotoxicity, we generated B16 cell lines that constitutively expressed high levels of PD1 or a mutant with a deletion of its intracytoplasmic domain (PD1ΔC) incapable of signal transduction (Figure 1D). Both B16-PD1 and B16-PD1ΔC cells significantly overcame the inhibitory effects of IFNβ expression, for which only the PD1 extracellular part, but not its intracytoplasmic signaling domain, was required. As expected, expression of IFNβ, together with PDL1 silencing, was still lethal to B16-PD1 and B16-PD1ΔC cells (Figure 1D). These results demonstrated the requirement of PDL1 to transmit a survival signal that is nevertheless potentiated by PD1 engagement.

To assess whether PDL1 possessed intrinsic signal transduction capacities that protected against IFNβ toxicity, B16 cells overexpressing a deletion mutant lacking the intracytoplasmic domain (B16-PDL1ΔC) were generated. This PDL1 mutant did not have the target sequence for μPDL1 and was efficiently expressed on the cell surface. Again, PDL1ΔC overexpression did not alter the surface expression of IFNAR1 (Figure 1E and not depicted). Unlike the wild-type version, the overexpression of PDL1ΔC did not overcome the lethality conferred by the co-expression of IFNβ with μPDL1 (Figure 1E). Considering these data, we concluded that PDL1 counteracts IFNβ cytotoxicity by signal transduction through its intracytoplasmic domain.

Conserved Motifs within the Intracytoplasmic Domain of PDL1 Regulate Protection from IFNβ Cytotoxicity

We then thoroughly analyzed the PDL1 intracytoplasmic domain using several bioinformatics tools. PDL1 presents a strongly amphiphilic intracytoplasmic domain without any obvious signaling domains (Figure S1). After extensive searches using different databases and algorithms, only MotifFinder produced a positive hit with a domain present in a bacterial and eukaryotic DNA-dependent RNA polymerase β subunit (Figure S1). No sequences related to signal transduction were found, suggesting that PDL1 is using non-conventional signaling motifs.

Therefore, to identify PDL1 signal transduction functional domains, we reasoned that these would be phylogenetically conserved. The intracytoplasmic regions of 10 mammalian PDL1 molecules were aligned, including the corresponding sequence from salmon as a divergent control (Figure 2A). Three conserved sequences were identified that we termed "RMLDVEKC," "DTSSK," and "QFEET" motifs. PDL1 undergoes ubiquitination, which leads to its destabilization (Lim et al., 2016), and we found that lysines 271 and 280 within RMLDVE<u>K</u>C and

---

error bars (SEM) after 2 weeks of puromycin selection following transduction of the indicated B16 cell lines (bottom of the graphs) with lentivectors co-expressing IFNβ-PuroR or IFNβ-μPDL1-PuroR. Data were obtained from 10 independent experiments.

(D) Left: flow cytometry histograms for PD1 surface expression in the indicated B16 cell lines on the right of the plots. Numbers and percentages indicate mean fluorescent intensities and percentage of positive cells. PD1ΔC indicates a PD1 protein lacking the intracytoplasmic signaling domain. Right: bar graphs representing the mean relative number of cells with error bars (SEM) after 2 weeks of puromycin selection following transduction of the indicated B16 cell lines (bottom of the graphs) with lentivectors co-expressing IFNβ-PuroR or IFNβ-μPDL1-PuroR. Data were obtained from 4 independent experiments.

(E) Flow cytometry histograms for surface expression of PDL1 (left) or IFNAR1 (right) on the indicated cell lines on the right of the plots. Numbers and percentages indicate mean fluorescent intensities and percentage of positive cells. PDL1ΔC, PDL1 protein without the intracytoplasmic region.

(F) Bar graphs representing the mean relative number of cells with error bars (SEM) after 2 weeks of puromycin selection following transduction of the indicated B16 cell lines (bottom of the graphs) with lentivectors co-expressing IFNβ-μPDL1-PuroR. Relevant statistical comparisons are indicated within the graphs from three independent experiments. Asterisks indicate very significant (**p < 0.01) and highly significant (***p < 0.001) differences.
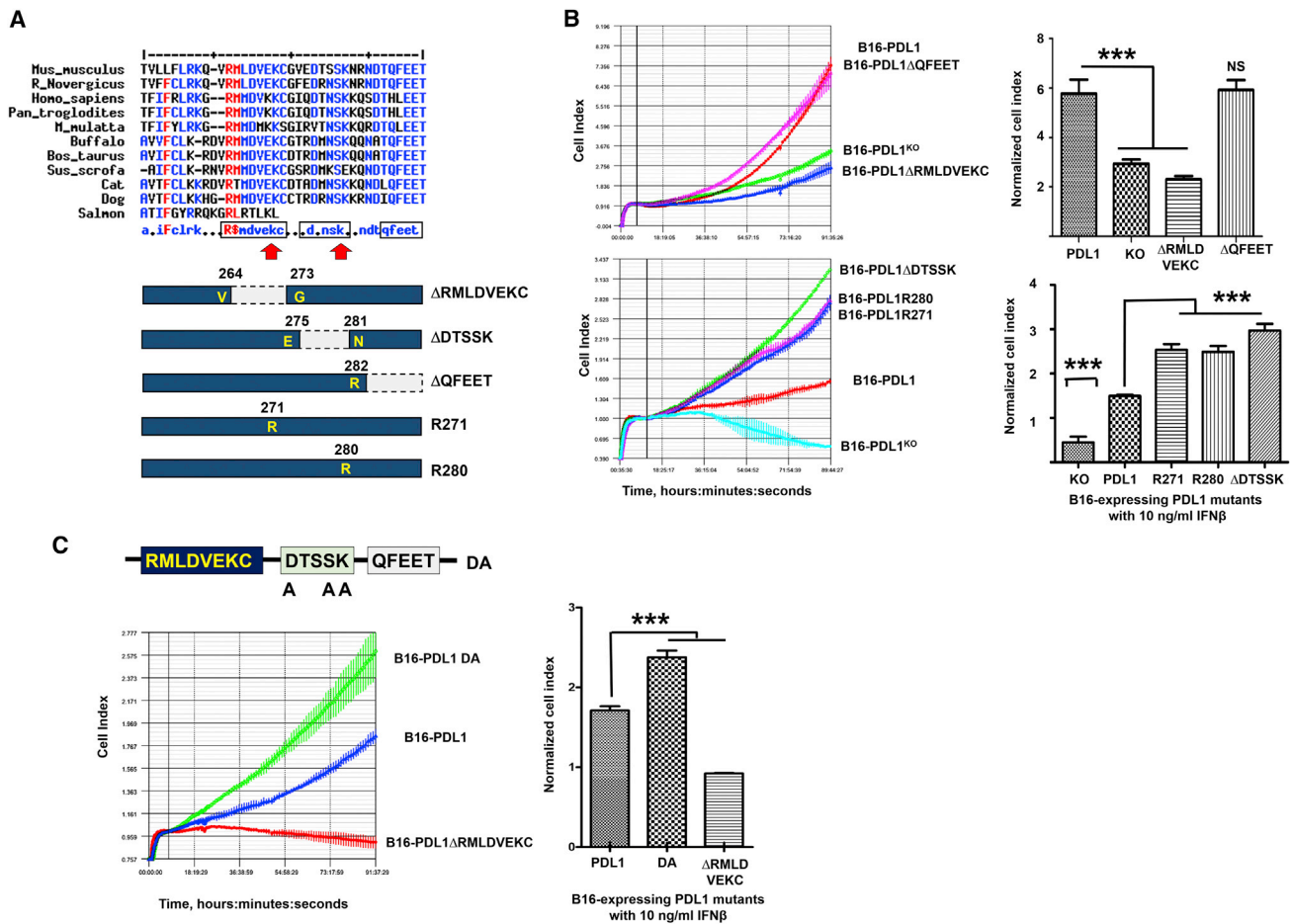
Figure 2. PDL1 Protection from IFNβ Cytotoxicity Is Regulated by Conserved Sequence Motifs

(A) Alignment of the intracytoplasmic domain from PDL1 molecules of the indicated species. In red and blue are highly conserved residues. The consensus sequence is shown on the bottom, with the three conserved motifs within open boxes. Lysines predicted to be capable of undergoing ubiquitination are indicated with arrows. Below the alignment are schemes indicating deletions or arginine substitutions.

(B) Left: real-time monitoring cell growth graphs from B16-PDL1^KO cells reconstituted with the deletion mutants shown in (A), as indicated. Data are shown as means from two independent cultures. Right: bar graphs plotting the cell index during the last 20 hr for each mutant as indicated, using means from duplicates as data for the analyses.

(C) As in (B) but using B16 cells expressing a PDL1 mutant with DSK residues mutated to alanines. Relevant statistical comparisons are indicated within the graph. ***p < 0.001, highly significant difference.

DTSS**K** motifs were putative targets for this post-translational modification according to the application of a random forest algorithm (Radivojac et al., 2010) (Figure 2A). To test the functionality of these domains, B16 cells lacking PDL1 (B16-PDL1^KO) were generated using CRISPR/Cas9 (Figure S2). Then, a PDL1 gene was constructed to prevent its cleavage by Cas9 through mutation of the CRISPR/Cas9 target site while conserving the wild-type amino acid sequence (PDL1wt). PDL1wt and mutants with deletions of each motif were expressed in B16-PDL1^KO cells (Figures 2A and S2). Two additional PDL1 mutants with conservative lysine-to-arginine substitutions were generated to eliminate the possibility of PDL1 undergoing ubiquitination within the intracytoplasmic domain (Figure 2A). All PDL1 mutants were efficiently transported and expressed on the cell surface, as assessed by flow cytometry following surface staining with PDL1-specific antibodies (Figure S2). Then, the inhibitory activities of recombinant

IFNβ over these B16 modified cell lines were tested by real-time monitoring of cell growth/viability (RTCA). An IFNβ concentration of 10 ng/mL was chosen, as it caused at least 50% growth inhibition of B16-PDL1wt cells as assessed by RTCA. CRISPR/Cas9 abrogation of PDL1 (B16-PDL1^KO) strongly sensitized B16 cells to recombinant IFNβ, even causing cell death (Figures 2B and 2C), in agreement with our initial observations based on IFNβ expression with a lentivector and also discarding potential off-target effects of μPDL1 (Figure 1). PDL1 with a deleted QFEET motif retained its protective capacities. In contrast, removal of the RMLDVEKC motif completely abrogated anti-IFNβ activity (Figure 2B). Interestingly, deletion of the DTSSK motif as well as lysine-to-arginine mutations within the RMLDVEKC or DTSSK motifs significantly enhanced resistance to IFNβ (Figure 2B). These results strongly suggested that DTSSK was a regulatory motif that modulates anti-IFN activity. To confirm this, the

conserved D, S, and K residues in the DTSSK motif were mutated to alanines, and the resulting PDL1 molecule was well expressed on the surface of B16-PDL1^{KO} cells (B16-DA cells). The alanine replacement of these residues showed an enhancement of the protective functions of PDL1 against IFNβ, strongly reinforcing the evidence that DTSSK is an inhibitory motif of PDL1's protective functions (Figure 2C).

Overall, we concluded that the RMLDVEKC motif is essential for PDL1's protection against IFNβ, while the DTSSK motif and the lysines 271 and 280 act as negative regulators.

STAT3-Caspase-7 Is the Main Effector Pathway Conferring IFNβ Lethality to PDL1 Silencing

Type I IFNs exert their activities by engaging with its receptor, IFNAR1/IFNAR2, on the cell surface. The main signal cascade depends on the recruitment of janus kinase 1 (JAK1) and TYK2, which phosphorylates signal transducer and activator of transcription (STAT)1, STAT2, and STAT3, which associate into STAT1/STAT2 heterodimers or STAT1/STAT1 and STAT3/STAT3 homodimers. In addition, type I IFNs cause caspase-dependent apoptosis, although the exact mechanisms are yet unclear. To identify the downstream effectors leading to exacerbated toxicity by lack of PDL1, B16 cell lines were generated with a selection of key components of the IFN signal transduction pathway silenced (Figure 3A).

These cell lines were tested in the IFNβ survival assay as described above (Figure 1). As expected, IFNAR1 and JAK1 silencing abrogated IFNβ toxicity. Interestingly, silencing of STAT3 and caspase-7 (CASP7) also reduced IFNβ inhibitory effects (Figure 3B). Moreover, lethality of the IFNβ-μPDL1 combination was only averted by silencing IFNAR1, JAK1, STAT3, and CASP7 (Figure 3C). To find out whether the absence of PDL1 signals enhanced IFNβ signal transduction, the expression of STATs was assessed in B16 and CRISPR/Cas9 PDL1 knockout B16 cells after IFNβ treatment for 24 hr (Figure 3D). STAT1 and STAT2 were upregulated to the same extent in B16 and PDL1^{KO} cells. In contrast, STAT3 levels increased only in PDL1^{KO} cells in response to IFNβ. Then, we performed a time-course assay of STAT3 phosphorylation after IFNβ stimulation. Interestingly, STAT3 Y705 phosphorylation was stronger and occurred faster in PDL1^{KO} cells, while STAT3 S727 phosphorylation remained unchanged in B16 and in B16-PDL1^{KO} cells (Figure 3E). These results indicated that PDL1 signals were inhibiting STAT3 Y705 phosphorylation and prevented STAT3 upregulation.

Survival assays with CASP-silenced B16 cell lines suggested that interference with PDL1 expression was causing cell death in response to IFNβ through CASP7. Our results also indicated that cell death was largely caused by apoptosis rather than CASP-independent necroptosis, although the participation of this last mechanism cannot be completely ruled out. To confirm these results, RTCA was performed with CASP-silenced B16 cells or CASP-silenced B16-PDL1^{KO} cell lines in response to recombinant IFNβ (Figure 3F). While CASP3 silencing did not abrogate toxicity to recombinant IFNβ, CASP7 silencing inhibited IFNβ inhibitory actions. The same results were also observed in B16-PDL1^{KO} cells, although in this assay, CASP9 silencing counteracted toxicity as well. Then, the expression

and processing of effector CASPs in B16 cells after treatment with recombinant IFNβ was compared to B16-PDL1^{KO} cells. Overall, basal expression of CASP3, 7, and 9 were increased in B16-PDL1^{KO} cells, especially after IFNβ treatment (Figure 3G). In agreement with the small hairpin RNA (shRNA) data, the processing of CASP7 was strongly enhanced in B16-PDL1^{KO} following IFNβ treatment (Figure 3F). Overall, these data suggested that the effector pathway for IFNβ cytotoxicity caused by PDL1 silencing was mainly mediated by a reinforced STAT3-CASP-7 pathway.

Antibody-Mediated PDL1 Blockade Abrogates the Protective Functions of PDL1 in Murine and Human Cancer Cell Lines

To test whether direct blockade of PDL1 could sensitize B16 and other murine and human cancer cells to IFNβ, the growth and viability of murine B16, CT26 colorectal, and 4T1 breast cancer cells were monitored by RTCA in the presence of increasing concentrations of a PDL1-blocking antibody or an isotype control (Figures 4A–4C). PDL1 antibody blockade sensitized all three murine cancer cell types to recombinant IFNβ. The same results were obtained with human B-RAF mutated melanoma HTB72 cells. Taken together, these results confirmed that the anti-IFNβ mechanism regulated by PDL1 is conserved in murine and human cancer cells.

Somatic Mutations in Human Cancers Targeting the DTSSK Domain Strongly Potentiate Global Anti-IFN Activities of PDL1

Our data strongly suggested that cancer cells rely on PDL1 signal transduction to counteract IFN toxicity. As this could be relevant for human immunotherapy, we studied the somatic mutations within the intracytoplasmic domain of PDL1 in human neoplastic malignancies. The catalogue of somatic mutations in cancer (COSMIC), ICGC, Intogen, and TCGA catalogs of somatic mutations in cancer were consulted, and several mutations leading to amino acid changes were identified in carcinomas, including skin and lung cancers. Interestingly, the majority of these (5 out of 7) directly affected the human homolog of the DTSSK motif (Figure 5A). To test the effects of these mutations over PDL1's protective functions, the two most disruptive mutations (D276H and K280N) were introduced into the equivalent murine PDL1 gene, and B16-PDL1^{KO} cells were transduced to express each mutant.

Then, RTCA was used to monitor the growth and survival of the B16 cell lines in the presence of recombinant IFNβ (Figure 5B), IFNα (Figure 5C), and IFNγ (Figure 5D). Consistent with our previous results, these mutations within the DTSSK motif strongly enhanced resistance to cytotoxicity mediated by type I and type II IFNs, while B16-PDL1^{KO} cells were highly sensitive to IFNα, IFNβ, and IFNγ. These results confirmed the regulatory role of the DTSSK motif by selection of variants in human carcinomas that disrupt its inhibitory activity leading to hyperactive PDL1 proteins. Moreover, these mutations extended wide protection from IFNα and IFNγ. Finally, the inhibitory activity of DTSSK was not exclusively dependent on lysine 280, as the D276H mutation also enhanced protective activity of PDL1.
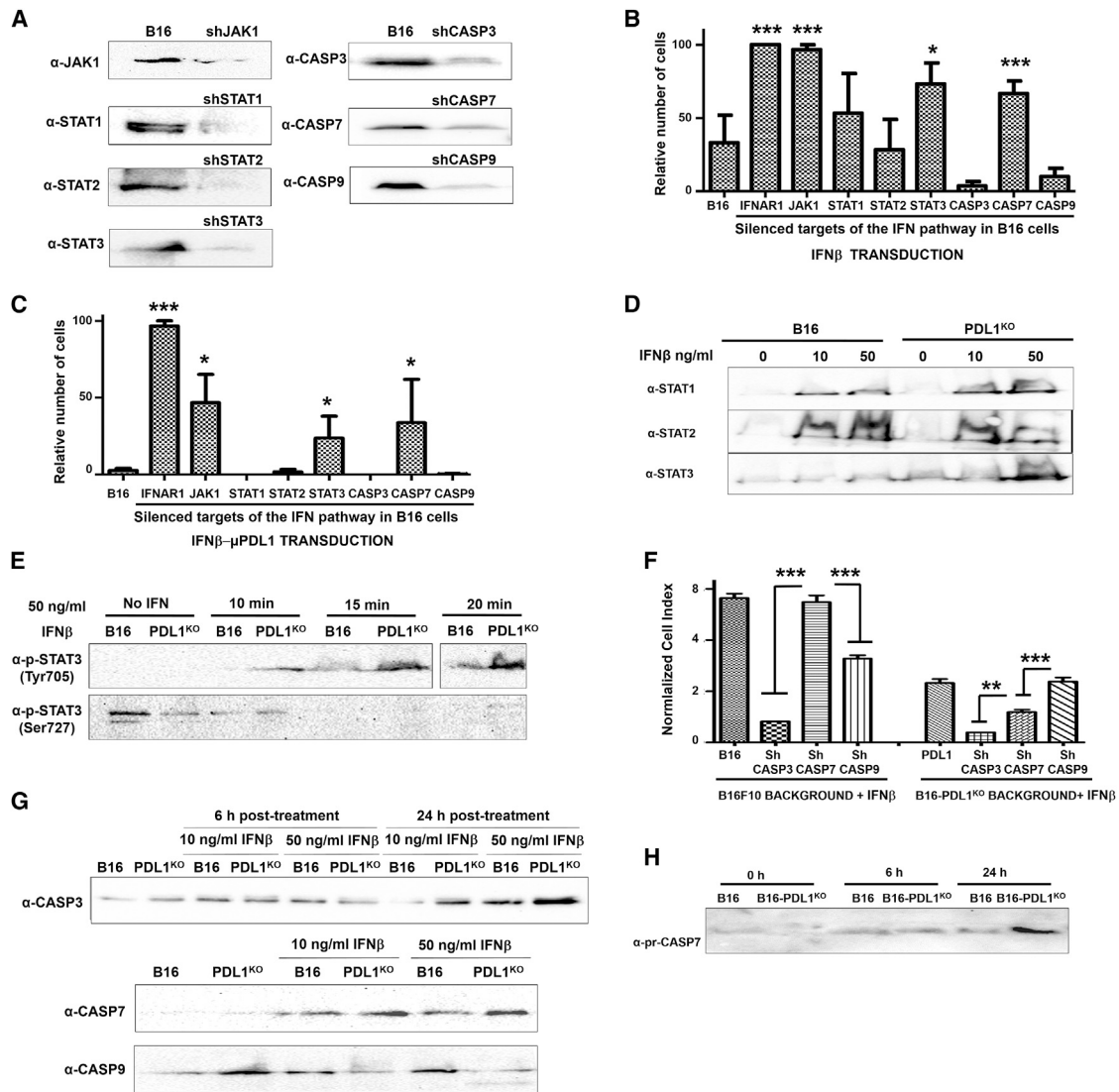
Figure 3. IFNβ-Enhanced Cytotoxicity by PDL1 Silencing Depends on a STAT3-CASP7 Pathway

(A) Western blots of the specific signal transduction molecules as shown on the left in B16 cell lines constitutively expressing the shRNAs indicated on top.

(B) Bar graphs representing the mean relative number of cells with error bars (SEM) after 2 weeks of puromycin selection following transduction of the indicated B16 cell lines (with the indicated silenced genes as shown) with lentivectors co-expressing IFNβ-PuroR.

(C) Same as in (B), but transductions were performed with lentivectors co-expressing IFNβ-μPDL1-PuroR.

(D) Detection by western blotting of the indicated STAT molecules in B16 or B16-PDL1^{KO} cells untreated or treated with IFNβ as shown on top.

(E) Western blot of STAT3 Y705 phosphorylation (top) at the indicated time points in B16 and B16-PDL1^{KO} cells after IFNβ stimulation, as indicated. Western blot (bottom) of STAT3 S727 phosphorylation in B16 or B16-PDL1^{KO} cells after IFNβ stimulation, as indicated.

(F) Bar graphs representing RTCA cell index of the indicated B16 cell lines with silenced CASPs either in an unmodified or PDL1^{KO} background as shown in the graphs in the presence of 10 ng/mL recombinant IFNβ.

(G) As in (D) but with detection of the indicated CASPs.

(H) Western blot of processed CASP7 on a time course of B16 or B16-PDL1^{KO} cells treated with 10 ng/mL recombinant IFNβ as shown on top. Relevant statistical comparisons are indicated within the graphs. Asterisks indicate significant (*p < 0.05), very significant (**p < 0.01), and highly significant differences (***p < 0.001).

PDL1 Signal Transduction in Cancer Cells Is Required for In Vivo Protection against IFNβ

Our data collectively suggested that PDL1 intrinsic signaling within cancer cells would confer resistance to IFNs in vivo independently of its inhibitory role over T cells. To prove this, we studied in vivo tumor growth from B16 cells in which PDL1 expression or signaling were altered, followed by intra-tumor administration

of IFNβ expressed by a lentivector or a GFP-expressing control. First, groups of mice were subcutaneously inoculated with B16, B16-PDL1, and B16 cells harboring a published PDL1-targeted shRNA, which reduced the basal expression of PDL1 (Broos et al., 2017) (Figure 6A). Then, lentivectors expressing either GFP (control) or IFNβ-GFP were injected into tumors 7 and 14 days later. Intra-tumor expression of IFNβ-GFP delayed
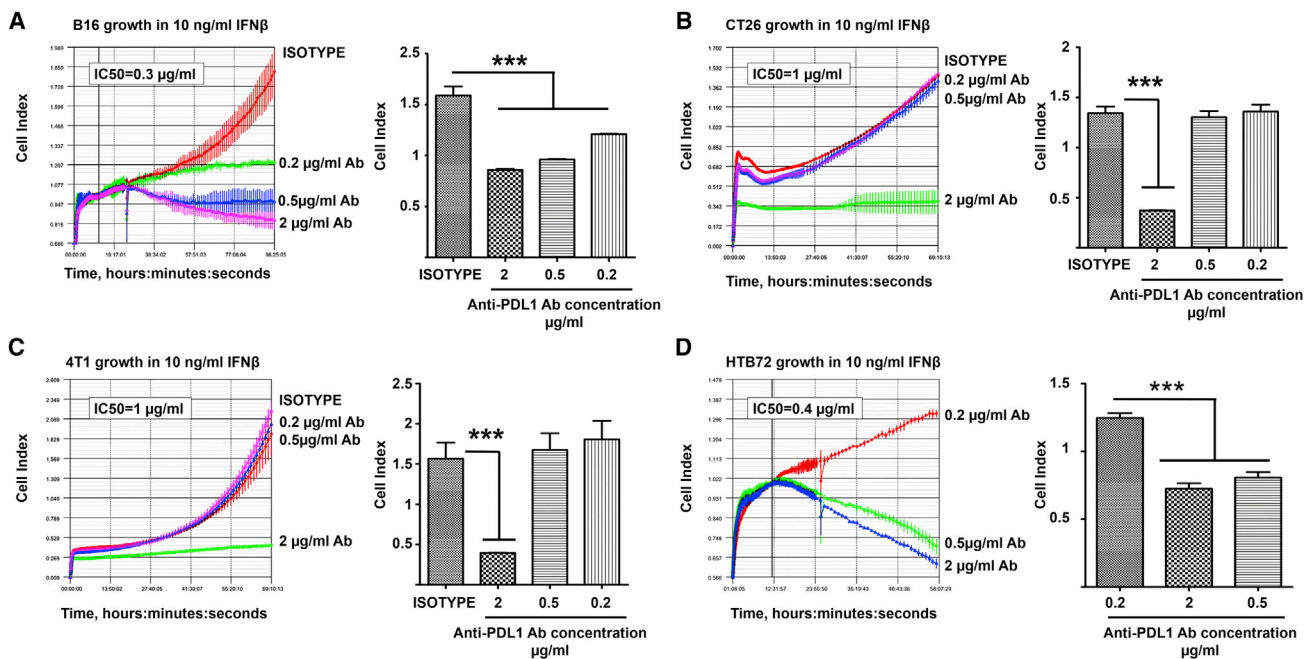
Figure 4. PDL1 Blockade Sensitizes Murine and Human Cancer Cells to IFNβ
(A) Left: RTCA graph of murine B16 melanoma cells in the presence of recombinant IFNβ and the indicated concentrations of anti-PDL1 antibody. Right: same data as a bar graph but with means and SD with error bars (n = 4).
(B) Same as (A) but with murine CT26 colorectal cancer cells.
(C) Same as (A) but with murine 4T1 breast cancer cells.
(D) Same as (A) but with human HTB72 melanoma cells. Calculated IC_{50} values are shown within the graphs. ***p < 0.001, highly significant difference.

B16 melanoma tumor growth (Figure 6A). PDL1 overexpression completely abrogated this sensitivity to IFNβ-GFP. In contrast, tumors arising from B16-shPDL1 were highly sensitive to LV-IFNβ-GFP, resulting in a significant delay in tumor growth and increased survival (Figure 6A). We repeated the experiment using B16-PDL1^{KO} cells. As expected, tumors arising from B16-PDL1^{KO} cells were highly responsive to intra-tumor lentivector delivery of IFNβ-GFP, leading to a highly significant increase in survival (Figure 6B). In fact, the lack of PDL1 was sufficient to delay tumor progression even in the absence of intratumor expression of IFNβ (Figure 6B).

These results showed a higher sensitivity in these B16 tumors to IFNβ when PDL1 expression was interfered with. However, inhibition of PDL1 expression in cancer cells could still enhance the cytotoxicity of T cells through reduced PDL1-PD1 engagement. Therefore, we carried out the same experiments but included a group in which B16-PDL1ΔC cells were inoculated. PDL1 in these cells can still engage PD1 on the surface of T cells but with impaired signal transduction within cancer cells (Figure 1). Then, tumors from B16, B16-PDL1, and B16-PDL1ΔC were inoculated with lentivectors expressing IFNβ-GFP. As expected, PDL1 overexpression in B16 cells very significantly counteracted the inhibitory effects of IFNβ and accelerated tumor progression (Figure 6C). In contrast, expression of PDL1ΔC did not confer resistance to intra-tumor delivery of IFNβ. As this mutant can still engage PD1 on T cells, these results indicate that PDL1 signal transduction contributes significantly to protection of cancer cells from type I IFNs. Overall, these results showed

that independently of its role in inhibiting cytotoxic T cells, PDL1 provides a first protective barrier to cancer cells by interfering with IFN signal transduction.

DISCUSSION

IFNs are known to exert anti-tumor effects, which include CASP-dependent apoptosis (Apelbaum et al., 2013), cell growth arrest (Vannucchi et al., 2000), and cell senescence (Katlinskaya et al., 2016; Yu et al., 2015). IFNs play a critical role in anti-cancer immune responses and contribute to the efficacy of conventional treatments and immunotherapies. There is ample evidence on the role that IFNs play in tumor repression, immune editing, and progression (Zitvogel et al., 2015). Many treatments, including chemotherapy and targeted therapies, need an intact IFN signal transduction pathway in cancer cells to exert their anti-tumor effects. However, type I IFNs in progressing tumors also drive immune editing (Smyth, 2005). In fact, acquisition of inactivating mutations affecting IFN signaling could be considered a core mechanism for tumor escape and progression. Recently, it has been shown that inactivating *JAK1*, *JAK2*, and β2-microglobulin mutations in cancer cells are responsible for primary and acquired resistance to anti-PD1 treatment in a cohort of patients (Shin et al., 2017; Zaretsky et al., 2016). The authors of these studies proposed that switching off IFN signal transduction prevented the adaptive PDL1 expression in cancer cells, becoming functionally PDL1 negative and refractory to PDL1/PD1 blockade. However, PDL1 itself can transmit signals without
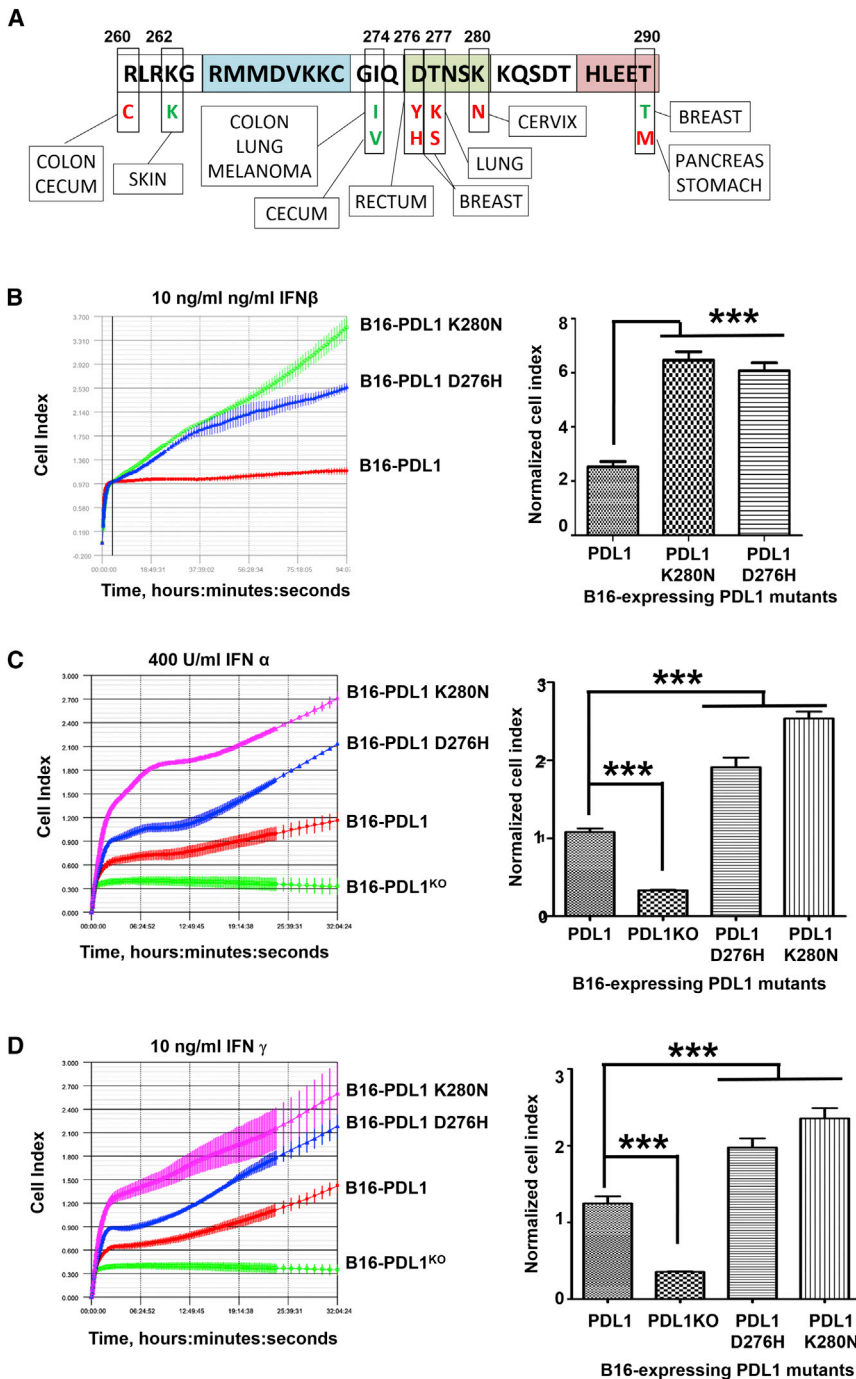
Figure 5. Somatic Mutations in the Human DTSSK Homolog Motif Lead to Hyperactive PDL1 Molecules that Protect Cells from Type I and Type II IFNs

(A) Schematics on the distribution of somatic mutations found within the intracytoplasmic domain of human PDL1. Blue, green, and red are used to show the homologous human RMLDVEKC, DTSSK, and QFEET motifs. Mutations are shown below, with conservative changes in green and non-conservative changes in red. The specific carcinomas for which mutations were described are indicated within boxes. Numbers represent amino acid positions in the murine and human PDL1 molecule.

(B) The two most disruptive mutations were introduced in the DTSSK murine motif and the resulting PDL1 molecules expressed in B16-PDL1^{KO} cells. Left: RTCA plot of the indicated B16 cell lines expressing the PDL1 mutants compared to PDL1wt in the presence of 10 ng/mL recombinant IFNβ. Right: the same data as bar graphs representing the mean of the normalized cell index from duplicate cultures, together with SDs as error bars.

(C) As in (B) but with IFNα. PDL1KO indicates B16 cells in which PDL1 was disrupted with CRISPR/Cas9.

(D) As in (B) but with IFNγ. Relevant statistical comparisons are indicated within the graph.
***p < 0.001, highly significant difference.

sion of PDL1, possibly as a negative feedback mechanism to regulate IFN signaling. It has to be taken into account that IFNs are potent transcriptional activators of PDL1 (Zaretsky et al., 2016).

PDL1 possesses a short intracytoplasmic region without any obvious known domains regulating signal transduction. However, it has been shown by others and us that there is PDL1 intrinsic signaling regulating cell growth, survival, and protection against apoptotic signals (Azuma et al., 2008; Clark et al., 2016; Chang et al., 2015; Liechtenstein et al., 2014a). We have identified functional regulatory sequence motifs within the intracytoplasmic domain responsible for PDL1 protection against IFN. The conserved RMLDVEKC motif is required to counteract IFNβ toxicity, while the

engaging PD1 or CD80 through mTOR (Clark et al., 2016; Chang et al., 2015). Here, we demonstrate that PDL1 signal transduction in murine and human cancer cells does in fact represent a barrier of protection against IFN cytotoxicity by inhibitory crosstalk with the type I IFN signal transduction pathway. It is important to emphasize that basal PDL1 expression reduces IFN cytotoxicity but does not completely abrogate it. Therefore, cancer cells respond to IFNs by upregulating the surface expres-

DTSSK motif and arginines 271 and 280 act as negative regulators of PDL1 functions. These sequences constitute non-classical signal transduction motifs, as they do not resemble any known signal transduction consensus. Only the sequence EKCGVEDTSSKNR shows high similarity to a domain in DNA-directed RNA polymerase subunit β, which interestingly includes the DTSSK motif (Figure S1). However, the relevance of this observation is unclear.
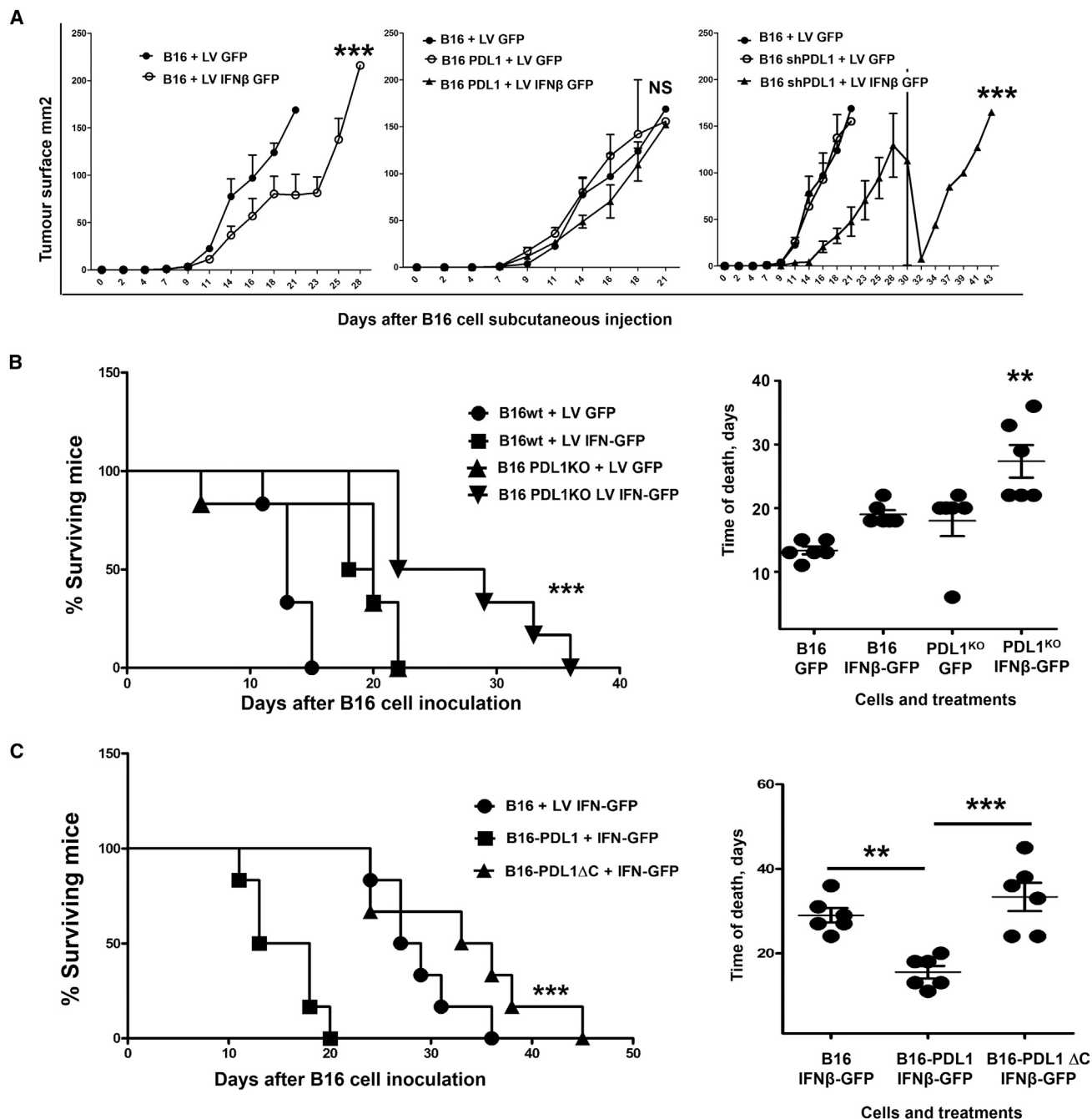
Figure 6. PDL1 Intrinsic Signaling in Cancer Cell Protects Tumors from IFNβ In Vivo

(A) Left: tumor growth graphs from injected B16 cells followed by intratumor injection with the indicated lentivectors, represented as means of tumor surfaces from groups of 6 mice with SDs as error bars. The middle and right graphs as in the left graph but using the indicated B16 cell lines overexpressing PDL1 (B16-PDL1) or B16 cell lines expressing a PDL1-targeted shRNA (B16-shPDL1).

(B) The growth graph as in (A) but using B16 wild-type or B16 PDL1 knockout cells. The graph on the right represents the time of death of each mouse from the data shown on the left graph. The cell lines and the injected lentivectors are shown on the bottom of the graph.

(C) Same as in (B) but using B16 wild-type, B16-PDL1, or B16-PDL1ΔC cells, which express a PDL1 mutant lacking the intracytoplasmic domain. Asterisks indicate very (**p < 0.05) and highly (***p < 0.001) significant differences.

Our findings also show that PD1 expression protects cancer cells from IFNβ toxicity by engaging PDL1. Hence, both PDL1 and PD1 blockade would sensitize cancer cells to IFN-mediated cytotoxicity. Furthermore, we found that antibody-mediated PDL1 blockade is sufficient to sensitize cancer cells to IFNs. Therefore, any adaptation of cancer cells to either inhibit the

IFN signaling pathway (Shin et al., 2017; Zaretsky et al., 2016) or potentiate PDL1 activities will favor their escape from the immune attack. Accordingly, a variety of human carcinomas select somatic mutations that affect residues within the inhibitory DTSSK motif, thereby increasing the anti-IFN activity of PDL1. These cancer cells with hyperactive PDL1 mutants are very likely selected in human malignancies as a result of immune editing.

Our data demonstrate that PDL1 signal transduction through conserved signaling motifs represents a protective barrier of cancer cells against IFN cytotoxicity, which would be reinforced by its inhibitory properties to T cells when engaged with PD1. A therapeutic approach such as PDL1/PD1 blockade would cause rapid cancer cell death due to further sensitization to IFN. This situation strongly favors the survival of variants resistant to IFN signal transduction. Therefore, cancer cells with mutated JAK1 or JAK2 kinases are intrinsically resistant to IFN toxicity and do not show adaptive PDL1 upregulation (Shin et al., 2017; Zaretsky et al., 2016).

EXPERIMENTAL PROCEDURES

Cells and Mice
HEK293T cells were purchased from the American Type Cell Culture Collection (ATCC). Murine melanoma B16F10 cells were grown as described previously (Liechtenstein et al., 2014a). Murine CT26 colorectal and 4T1 breast cancer cells were grown in DMEM. Human HTB72 cells were grown in RPMI. C57BL/6 female mice were purchased from The Jackson Laboratory. Approval for animal studies was obtained from the Animal Ethics Committee of the University of Navarra (Pamplona, Navarra, Spain) and from the Government of Navarra. When indicated, recombinant IFNβ was added to the cell cultures at the appropriate concentrations. Cell growth and survival were monitored in real time using the xCELLigence real-time cell analysis system (RTCA, ACEA Biosciences) by seeding between 3,000 and 10,000 cells as required, in the presence or absence of recombinant IFNβ. Inhibitory concentration 50 (IC$_{50}$) was calculated by RTCA for B16 cell lines with increasing concentrations of recombinant IFNβ. Experiments of antibody-mediated PDL1 blockade were carried out with anti-PD-L1 monoclonal antibody (clone 10B5) (Dong et al., 2002). For human PDL1 blockade, the in-house phage-display engineered humanized immunoglobulin G1 (IgG1) recombinant antibody Plimilumab was used.

Plasmids
The FB2 fusokine transgene is described in (Van der Jeught et al., 2014) and consists on a fusion gene between the murine IFNβ and the ectodomain of the TGFβ receptor II. The FB2 transgene was cloned into the pDUAL-p1-PuroR vector by standard cloning techniques. This vector contains a PDL1-targeted microRNA and has been described previously (Liechtenstein et al., 2014a). The IFNβ coding sequence was amplified by PCR and cloned into pDUAL-μPDL1-PuroR and pDUAL-GFP (Liechtenstein et al., 2014a). Likewise, the TGFβRII was amplified by PCR, introducing the IFNβ signal peptide for secretion at the 5′ end, and cloned into pDUAL-p1-PuroR. When required, the same transgenes were expressed without the PDL1-targeted microRNA. The pHIV-SIREN lentivectors (Lanna et al., 2014; Liechtenstein et al., 2014b) were used to express shRNAs targeting the indicated genes (Table S1) together with blasticidin resistance. The PDL1 transgene was ordered from Geneart and includes 7 silent mutations (ccaaagatctttatg, mutations underlined) and 6 silent mutations (agaaacgacacgcagttt) at the amino and C termini to prevent its silencing by either μPDL1 or PDL1-targeted CRISP/CAS9. PDL1ΔC encodes a C-terminal deleted PDL1 gene and was generated by PCR using forward (FW; ggatccgccaccatgaggatatttgctggc) and reverse (RS; cggccgcttattg ttttctcaagaagaggaggaccg) oligos. PDL1-deletion and single-point substitution mutants were generated by overlap-extension PCR as described (Escors et al., 2001) using the PDL1 gene as a template and the indicated oligonucleotides (Table S2). The murine PD1 transgene was ordered from Geneart and

cloned into pDUAL-BlastR, which expresses blasticidin resistance under the control of the ubiquitin promoter. A C-terminal-deleted version was also generated by PCR using FW (gggggggatccgccaccatgtgggtccggcaggtacc) and RS (gcggccgcttatgagcagaagacagctagggccaggc) oligos, followed by cloning into pDUAL-BlastR.

The mouse CD274 (PDL1) sgRNA CRISPR/Cas9 "All-in-One" lentiviral transfer vector was used to knock out PDL1 as described previously (Broos et al., 2017).

Lentivector Production, Cell Transduction, and Generation of B16 Knockdown Stable Cell Lines
Lentivector production and titration were carried out as described elsewhere (Karwacz et al., 2011; Liechtenstein et al., 2014a; Selden et al., 2007). Transduction of the indicated cell lines was carried out with a multiplicity of transduction of 10, and transduced cells were selected with the appropriate concentration of either puromycin (Gibco) or blasticidin (Gibco). Transduced cells are then analyzed for the expression of the target of interest either by flow cytometry or western blot.

Western Blotting
Western blots were performed as described previously (Escors et al., 2008). Polyclonal anti-CASP-3, 7, 9 and anti-processed CASP-3, 7, and 9 and anti-phosphorylated STAT3 molecules were purchased from Cell Signaling Technology. Mouse anti-JAK1, STAT1, STAT2, and STAT3 antibodies were purchased from Cell Signaling Technology and anti-GADPH from Calbiochem. Peroxidase-conjugated polyclonal anti-mouse and anti-rabbit antibodies were purchased from DAKO and Cell Signaling Technology.

Cell Staining and Flow Cytometry
Surface and intracellular staining were performed as described previously (Escors et al., 2008) using the indicated antibodies. Phycoerythrin (PE)-Cy7-conjugated streptavidin, antigen presenting cell (APC)-conjugated streptavidin, PE-conjugated anti-IFNARI were purchased from BioLegend. PE-and fluorescein isothiocyanate (FITC)-conjugated streptavidin from Invitrogen. Biotin-conjugated anti-PDL1 was purchased from eBioscience. APC-conjugated anti-PD1 was purchased from Miltenyi Biotec.

B16-IFNβ Cell Survival Assays
The goal of this assay is to quantify viable growing B16 cell lines that constitutively express IFNβ following lentivector transduction with IFNβ-PuroR or IFNβ-μPDL1-PuroR followed by selection with puromycin. For this assay, 100,000 of the indicated transduced or non-transduced cells were plated in 6-well culture plates in triplicate. Cells were then transduced at a multiplicity of transduction of 10. One well was left as a non-transduced control. The next day, puromycin was added at 1 μg/mL, and surviving cells were allowed to grow for 2 weeks. Surviving cells were quantified and represented as a percentage compared to the growth of non-transduced, non-treated cells.

IFN Treatment of PDL1 Mutants and Real-Time Living Cell Monitoring
The appropriate cell types were seeded at a density of 5,000 cells per well on two L8 cell culture chambers for xCELLingence RTCA monitoring system (ACEA Biosciences). Cells were grown in DMEM or RPMI medium with recombinant murine or human IFNβ (10 ng/mL, eBioscience) as required. Murine IFNα (400 U/mL) and IFNγ (10 ng/mL) were purchased from (PeproTech). Growth and survival of cell lines were monitored by RTCA for a minimum of 3 days.

Vaccination and Tumor Experiments
Experiments were usually performed with six C57BL/6 mice per group. Mice were subcutaneously inoculated with 10^6 of the indicated B16 cell lines. Tumor size was monitored every 2 days. When required, tumors were injected with 10^6 lentivector transducing particles expressing IFNβ-GFP or with GFP only as a control. Mice were sacrificed when tumor surface was above 150 mm^2.

In Silico Sequence Analyses

PDL1 protein sequences from mouse, human, pig, cow, buffalo, cat, dog, and salmon were aligned using the multialign tool (http://multalin.toulouse.inra.fr/multalin/) (Corpet, 1988). Prediction of ubiquitination sites was performed with the UbPred tool (http://www.ubpred.org/) (Radivojac et al., 2010). The search for conserved protein domains was performed with MotifFinder (http://www.genome.jp/tools-bin/search_motif_lib). The data on somatic mutations in PDL1 from human cancers were obtained from the COSMIC (http://cancer.sanger.ac.uk/cosmic) and TCGA (https://cancergenome.nih.gov/) databases. The following mutations were found: R260C (colon and cecum carcinoma; COSU3769), R262K (basal cell carcinoma; COSP39263), I274I (lung, cecum carcinoma, and melanoma; COSP29675, COSU540, and COSU17), I274V (colon carcinoma, COSU144), D276H (breast invasive carcinoma; TCGA-AR-A0TX-01 and COSU414), D276Y (rectum carcinoma), T277K (George et al., 2015) (small cell lung cancer; COSP40339), T277S (lung carcinoma; COSP40399), K280N (cervical squamous cell carcinoma; TCGA-FU-A3HZ-01 and COSU415), T290M (pancreas and stomach carcinomas; TCGA-BR-4362-01 and COSU541), and T290T (breast cancer; COSU541).

Statistical Analyses

GraphPad Prism was used for plotting data and statistical analyses. No data were considered outliers. Data from the B16-IFNβ survival assay were confirmed to be normally distributed and therefore analyzed by two-way ANOVAs with a random criterion (inter-experiment variability). Two pair comparisons were carried out following the ANOVA analyses using either Bonferroni or Tukey's tests. Tumor growth and survival data were analyzed as described before (Karwacz et al., 2011). ACEA RTCA cell index data were analyzed for each sample in duplicate and plotted as means and SD. The data were highly homogeneous and normally distributed. For statistical analyses, the cell index data were collected at 75, 80, 85, and 90 hr of cell growth. The data were analyzed by two-way ANOVA with time as a random criterion followed by Tukey's pairwise comparisons.

ACCESSION NUMBERS

The accession numbers for the original flow cytometry data reported in this paper are Flow Repository: FR-FCM-ZY8H and Flow Repository: FR-FCM-ZY8W.

SUPPLEMENTAL INFORMATION

Supplemental Information includes two figures and two tables and can be found with this article online at http://dx.doi.org/10.1016/j.celrep.2017.07.075.

AUTHOR CONTRIBUTIONS

M.G.-C. designed and executed most of the experiments and analyzed the data. M.Z., H.A., M.I.-V., and G.F.-H. performed the experiments and analyzed the data. L.L. generated B16 cells lines overexpressing PD1. C.S., E.M., D.L., R.M., P.S., I.A., and C.W. contributed to PDL1-antibody blockade experiments. R.V. contributed to the analysis of clinical data and supervision of H.A. and G.F.-H. K.B. generated the interferon constructs. G.K. and D.E. supervised the project, planned and executed experiments, and analyzed the data. All authors contributed to the writing of the paper.

ACKNOWLEDGMENTS

REFERENCES

Apelbaum, A., Yarden, G., Warszawski, S., Harari, D., and Schreiber, G. (2013). Type I interferons induce apoptosis by balancing cFLIP and caspase-8 independent of death ligands. Mol. Cell. Biol. *33*, 800–814.

Azuma, T., Yao, S., Zhu, G., Flies, A.S., Flies, S.J., and Chen, L. (2008). B7-H1 is a ubiquitous antiapoptotic receptor on cancer cells. Blood *111*, 3635–3643.

Broos, K., Keyaerts, M., Lecocq, Q., Renmans, D., Nguyen, T., Escors, D., Liston, A., Raes, G., Breckpot, K., and Devoogdt, N. (2017). Non-invasive assessment of murine PD-L1 levels in syngeneic tumor models by nuclear imaging with nanobody tracers. Oncotarget *8*, 41932–41946.

Butte, M.J., Keir, M.E., Phamduy, T.B., Sharpe, A.H., and Freeman, G.J. (2007). Programmed death-1 ligand 1 interacts specifically with the B7-1 costimulatory molecule to inhibit T cell responses. Immunity *27*, 111–122.

Chang, C.H., Qiu, J., O'Sullivan, D., Buck, M.D., Noguchi, T., Curtis, J.D., Chen, Q., Gindin, M., Gubin, M.M., van der Windt, G.J., et al. (2015). Metabolic competition in the tumor microenvironment is a driver of cancer progression. Cell *162*, 1229–1241.

Clark, C.A., Gupta, H.B., Sareddy, G., Pandeswara, S., Lao, S., Yuan, B., Drerup, J.M., Padron, A., Conejo-Garcia, J., Murthy, K., et al. (2016). Tumor-intrinsic PD-L1 signals regulate cell growth, pathogenesis, and autophagy in ovarian cancer and melanoma. Cancer Res. *76*, 6964–6974.

Corpet, F. (1988). Multiple sequence alignment with hierarchical clustering. Nucleic Acids Res. *16*, 10881–10890.

Dong, H., Strome, S.E., Salomao, D.R., Tamura, H., Hirano, F., Flies, D.B., Roche, P.C., Lu, J., Zhu, G., Tamada, K., et al. (2002). Tumor-associated B7-H1 promotes T-cell apoptosis: a potential mechanism of immune evasion. Nat. Med. *8*, 793–800.

Escors, D., Ortego, J., Laude, H., and Enjuanes, L. (2001). The membrane M protein carboxy terminus binds to transmissible gastroenteritis coronavirus core and contributes to core stability. J. Virol. *75*, 1312–1324.

Escors, D., Lopes, L., Lin, R., Hiscott, J., Akira, S., Davis, R.J., and Collins, M.K. (2008). Targeting dendritic cell signaling to regulate the response to immunization. Blood *111*, 3050–3061.

Fife, B.T., Pauken, K.E., Eagar, T.N., Obu, T., Wu, J., Tang, Q., Azuma, M., Krummel, M.F., and Bluestone, J.A. (2009). Interactions between PD-1 and PD-L1 promote tolerance by blocking the TCR-induced stop signal. Nat. Immunol. *10*, 1185–1192.

Freeman, G.J., Long, A.J., Iwai, Y., Bourque, K., Chernova, T., Nishimura, H., Fitz, L.J., Malenkovich, N., Okazaki, T., Byrne, M.C., et al. (2000). Engagement of the PD-1 immunoinhibitory receptor by a novel B7 family member leads to negative regulation of lymphocyte activation. J. Exp. Med. *192*, 1027–1034.

George, J., Lim, J.S., Jang, S.J., Cun, Y., Ozretić, L., Kong, G., Leenders, F., Lu, X., Fernández-Cuesta, L., Bosco, G., et al. (2015). Comprehensive genomic profiles of small cell lung cancer. Nature *524*, 47–53.

Hodi, F.S., Hwu, W.J., Kefford, R., Weber, J.S., Daud, A., Hamid, O., Patnaik, A., Ribas, A., Robert, C., Gangadhar, T.C., et al. (2016). Evaluation of immune-related response criteria and RECIST v1.1 in patients with advanced melanoma treated with pembrolizumab. J. Clin. Oncol. *34*, 1510–1517.

Karwacz, K., Bricogne, C., MacDonald, D., Arce, F., Bennett, C.L., Collins, M., and Escors, D. (2011). PD-L1 co-stimulation contributes to ligand-induced T cell receptor down-modulation on CD8+ T cells. EMBO Mol. Med. *3*, 581–592.

Katlinskaya, Y.V., Katlinski, K.V., Yu, Q., Ortiz, A., Beiting, D.P., Brice, A., Davar, D., Sanders, C., Kirkwood, J.M., Rui, H., et al. (2016). Suppression of type I interferon signaling overcomes oncogene-induced senescence and mediates melanoma development and progression. Cell Rep. *15*, 171–180.

Lanna, A., Henson, S.M., Escors, D., and Akbar, A.N. (2014). The kinase p38 activated by the metabolic regulator AMPK and scaffold TAB1 drives the senescence of human T cells. Nat. Immunol. *15*, 965–972.

Liechtenstein, T., Perez-Janices, N., Blanco-Luquin, I., Goyvaerts, C., Schwarze, J., Dufait, I., Lanna, A., Ridder, M., Guerrero-Setas, D., Breckpot, K., and Escors, D. (2014a). Anti-melanoma vaccines engineered to simultaneously modulate cytokine priming and silence PD-L1 characterized using ex vivo myeloid-derived suppressor cells as a readout of therapeutic efficacy. OncoImmunology *3*, e945378.

Liechtenstein, T., Perez-Janices, N., Gato, M., Caliendo, F., Kochan, G., Blanco-Luquin, I., Van der Jeught, K., Arce, F., Guerrero-Setas, D., Fernandez-Irigoyen, J., et al. (2014b). A highly efficient tumor-infiltrating MDSC differentiation system for discovery of anti-neoplastic targets, which circumvents the need for tumor establishment in mice. Oncotarget *5*, 7843–7857.

Lim, S.O., Li, C.W., Xia, W., Cha, J.H., Chan, L.C., Wu, Y., Chang, S.S., Lin, W.C., Hsu, J.M., Hsu, Y.H., et al. (2016). Deubiquitination and stabilization of PD-L1 by CSN5. Cancer Cell *30*, 925–939.

Radivojac, P., Vacic, V., Haynes, C., Cocklin, R.R., Mohan, A., Heyen, J.W., Goebl, M.G., and Iakoucheva, L.M. (2010). Identification, analysis, and prediction of protein ubiquitination sites. Proteins *78*, 365–380.

Ragimbeau, J., Dondi, E., Alcover, A., Eid, P., Uzé, G., and Pellegrini, S. (2003). The tyrosine kinase Tyk2 controls IFNAR1 cell surface expression. EMBO J. *22*, 537–547.

Selden, C., Mellor, N., Rees, M., Laurson, J., Kirwan, M., Escors, D., Collins, M., and Hodgson, H. (2007). Growth factors improve gene expression after lentiviral transduction in human adult and fetal hepatocytes. J. Gene Med. *9*, 67–76.

Sharma, P., Hu-Lieskovan, S., Wargo, J.A., and Ribas, A. (2017). Primary, adaptive, and acquired resistance to cancer immunotherapy. Cell *168*, 707–723.

Sharpe, A.H., Wherry, E.J., Ahmed, R., and Freeman, G.J. (2007). The function of programmed cell death 1 and its ligands in regulating autoimmunity and infection. Nat. Immunol. *8*, 239–245.

Shin, D.S., Zaretsky, J.M., Escuin-Ordinas, H., Garcia-Diaz, A., Hu-Lieskovan, S., Kalbasi, A., Grasso, C.S., Hugo, W., Sandoval, S., Torrejon, D.Y., et al. (2017). Primary resistance to PD-1 blockade mediated by JAK1/2 mutations. Cancer Discov. *7*, 188–201.

Smyth, M.J. (2005). Type I interferon and cancer immunoediting. Nat. Immunol. *6*, 646–648.

Van der Jeught, K., Joe, P.T., Bialkowski, L., Heirman, C., Daszkiewicz, L., Liechtenstein, T., Escors, D., Thielemans, K., and Breckpot, K. (2014). Intratumoral administration of mRNA encoding a fusokine consisting of IFN-β and the ectodomain of the TGF-β receptor II potentiates antitumor immunity. Oncotarget *5*, 10100–10113.

Vannucchi, S., Percario, Z.A., Chiantore, M.V., Matarrese, P., Chelbi-Alix, M.K., Fagioli, M., Pelicci, P.G., Malorni, W., Fiorucci, G., Romeo, G., and Affabris, E. (2000). Interferon-beta induces S phase slowing via up-regulated expression of PML in squamous carcinoma cells. Oncogene *19*, 5041–5053.

Yu, Q., Katlinskaya, Y.V., Carbone, C.J., Zhao, B., Katlinski, K.V., Zheng, H., Guha, M., Li, N., Chen, Q., Yang, T., et al. (2015). DNA-damage-induced type I interferon promotes senescence and inhibits stem cell function. Cell Rep. *11*, 785–797.

Zak, K.M., Kitel, R., Przetocka, S., Golik, P., Guzik, K., Musielak, B., Dömling, A., Dubin, G., and Holak, T.A. (2015). Structure of the complex of human programmed death 1, PD-1, and its ligand PD-L1. Structure *23*, 2341–2348.

Zaretsky, J.M., Garcia-Diaz, A., Shin, D.S., Escuin-Ordinas, H., Hugo, W., Hu-Lieskovan, S., Torrejon, D.Y., Abril-Rodriguez, G., Sandoval, S., Barthly, L., et al. (2016). Mutations associated with acquired resistance to PD-1 blockade in melanoma. N. Engl. J. Med. *375*, 819–829.

Zitvogel, L., Galluzzi, L., Kepp, O., Smyth, M.J., and Kroemer, G. (2015). Type I interferons in anticancer immunity. Nat. Rev. Immunol. *15*, 405–414.